



**Harmonic quiet-day  
curves as  
magnetometer  
baselines**

M. van de Kamp

# Harmonic quiet-day curves as magnetometer baselines for ionospheric current analyses

**M. van de Kamp**

Finnish Meteorological Institute, P.O. Box 503, 00101 Helsinki, Finland

Received: 28 February 2013 – Accepted: 8 March 2013 – Published: 18 March 2013

Correspondence to: M. van de Kamp (kampmax@fmi.fi)

Published by Copernicus Publications on behalf of the European Geosciences Union.

[Title Page](#)

[Abstract](#)

[Introduction](#)

[Conclusions](#)

[References](#)

[Tables](#)

[Figures](#)



[Back](#)

[Close](#)

[Full Screen / Esc](#)

[Printer-friendly Version](#)

[Interactive Discussion](#)



## Abstract

This paper presents a novel method to determine a baseline for magnetometer data. This baseline consists of all magnetic field components not related to ionospheric and magnetospheric disturbances, i.e. all field components due to solar quiet variations and other background variations, as well as equipment effects. Extraction of this baseline is useful when the disturbance magnetic field is analysed. The full baseline is composed of two main constituents: the diurnal baseline and the long-term baseline.

For the diurnal baseline, first “templates” are derived, based on the lowest few harmonics of the daily curves from the quietest days. The diurnal variation of the baseline is obtained by interpolating between these templates. This method ensures a smooth baseline at all times, avoiding any discontinuities at transitions between days.

The long-term baseline is obtained by interpolating between the daily median values. This way, the baseline is ensured to follow long-term trends, such as seasonal and tidal variations, as well as equipment drift. The daily median values are calculated for all days except the most disturbed ones; a procedure is included to ensure that the median values used are unaffected by disturbances.

This procedure avoids many problems associated with other existing baseline procedures, and makes magnetometer data suitable, for instance, for the calculation of ionospheric equivalent currents related to geomagnetic storms. Even data from remote unmanned magnetometers, which exhibit significant equipment effects, can be made suitable this way, which can give valuable contributions to the equivalent current database.

GID

3, 87–125, 2013

## Harmonic quiet-day curves as magnetometer baselines

M. van de Kamp

[Title Page](#)

[Abstract](#)

[Introduction](#)

[Conclusions](#)

[References](#)

[Tables](#)

[Figures](#)

[⏪](#)

[⏩](#)

[◀](#)

[▶](#)

[Back](#)

[Close](#)

[Full Screen / Esc](#)

[Printer-friendly Version](#)

[Interactive Discussion](#)



# 1 Introduction

## 1.1 Equivalent currents

5 Currents flowing in the ionosphere are related to the field-aligned currents in the magnetosphere through ionosphere-magnetosphere coupling (e.g. Kamide and Baumjohann, 1993). The magnetospheric currents are strongly dependent on solar activity, such as solar wind variations and solar storms, and these solar-dependent magnetospheric current variations are also reflected to the ionospheric currents. Since strong disturbances in the ionospheric currents can affect technological systems on the ground (e.g. Boteler et al., 1998), there is a great interest in the dynamics of these  
10 currents in relation to solar activity.

The concept of ionospheric “equivalent currents” models the ionospheric currents as present in a thin shell, usually the highly conductive E-layer at 100 km height, and representing only the divergence-free, horizontal part of the total currents. Under many  
15 circumstances these give valuable information about spatial and temporal characteristics of the actual 3-D ionospheric currents (e.g. Untiedt and Baumjohann, 1993), especially when analysed together with data from other instruments, such as rockets, satellites, or radars. The short-term variations of the equivalent currents can effectively be estimated from magnetometer measurements from a two-dimensional ground-based magnetometer network.

20 The European Cluster Assimilation Technology (ECLAT) project funded by the EU FP7 programme provides a selection of useful supporting data sets to the Cluster Active Archive (Laakso et al., 2009). The work described in this paper has been used in an ECLAT work package in which ionospheric equivalent current vectors are computed in the Fennoscandia region from data from the ground magnetometer network IMAGE. These source data are described in the next subsection. In the project,  
25 equivalent currents are to be analysed for an area over Fennoscandia, over the period 2001–2010. An important motivation for publishing this paper is to provide for the

## Harmonic quiet-day curves as magnetometer baselines

M. van de Kamp

[Title Page](#)

[Abstract](#)

[Introduction](#)

[Conclusions](#)

[References](#)

[Tables](#)

[Figures](#)



[Back](#)

[Close](#)

[Full Screen / Esc](#)

[Printer-friendly Version](#)

[Interactive Discussion](#)



ECLAT database users accurate information about the equivalent current generation procedure used in the service.

For the equivalent current estimate, use is made of the method of spherical elementary current systems (Amm and Viljanen, 1999; Pulkkinen et al., 2003). The currents induced inside the earth are ignored, as they can be assumed to be relatively small compared to the ionospheric currents. For the calculation, only the  $x$ - (north) and  $y$ - (east) components of the magnetic field at all ground stations are necessary, as only these are related to the divergence-free part of the ionospheric currents.

## 1.2 IMAGE magnetometer measurements

The input data for the calculation of the ionospheric currents in the project ECLAT are the magnetometer recordings of the ground magnetometer network IMAGE (<http://space.fmi.fi/image/beta/>) (Viljanen and Häkkinen, 1997). This network consists of 32 magnetometers over geographic latitudes from 58 to 79 degrees, which is especially favourable for electrojet studies. The magnetometers return data at a time resolution of 10 s.

Figure 1 shows a map of the locations of the magnetometers of the IMAGE Network.

## 1.3 Various magnetic field components; baselines

In addition to the currents caused by solar and magnetospheric disturbances, which are of interest for the analysis, the ionospheric currents and the ground magnetic field consist of several other components.

The magnetic field measured at the earth's surface is a superposition of the field originating from the inner earth, and that from electromagnetic effects caused by the ionospheric currents. These ionospheric currents, in turn, contain on the one hand components due to the dynamo effect of the revolving magnetic earth inside the conducting ionosphere, whose conductivity depends (among others) on solar radiation, and on the other hand components caused by Coronal Mass Ejections and other disturbances in

### Harmonic quiet-day curves as magnetometer baselines

M. van de Kamp

[Title Page](#)

[Abstract](#)

[Introduction](#)

[Conclusions](#)

[References](#)

[Tables](#)

[Figures](#)

[⏪](#)

[⏩](#)

[◀](#)

[▶](#)

[Back](#)

[Close](#)

[Full Screen / Esc](#)

[Printer-friendly Version](#)

[Interactive Discussion](#)



solar activity via ionosphere-magnetosphere coupling, which are the components of interest for the ionospheric studies.

As a consequence, in the measured magnetic field the following variations of different time scales can be distinguished:

- The diurnal variations caused by the variation of ionospheric conductivity due to solar radiation during quiet times, usually referred to as “ $S_q$  variations” or “Solar quiet variations”.
- Lunar variations: variations over a lunar day (24 h and 50 min), due to changes in the global distribution of the conducting ionosphere due to lunar attraction. These are usually referred to as “ $L$  variations”.
- Seasonal variations: variations with a period length of one year, due to seasonal changes in the ionospheric conductivity (i.e. slow component of  $S_q$  variations), but also seasonal changes in the ionosphere-thermosphere-magnetosphere interactions.
- Secular (long-term) variations, due to very slow variations in the earth’s internal magnetic field pattern.
- The “disturbance field”, which, although irregular in nature, also shows statistical variations with time of day, season, and solar activity.
- In addition to the various field variation components, some magnetometer data also contain system effects such as equipment drift (see later).

Note that lunar, seasonal and secular variations are within the time range of days much smaller than the solar quiet variations and the disturbance field. The various components of the ground magnetic field are clearly explained by Chapman and Bartels (1940). Campbell (1989) gave an introduction on the physics of  $S_q$  and  $L$  variations and a short overview of the research history of these, as an editorial to a special issue of *Pure and Applied Geophysics*, dedicated to  $S_q$  and  $L$  variations.

**Harmonic quiet-day curves as magnetometer baselines**

M. van de Kamp

[Title Page](#)

[Abstract](#)

[Introduction](#)

[Conclusions](#)

[References](#)

[Tables](#)

[Figures](#)

[⏪](#)

[⏩](#)

[◀](#)

[▶](#)

[Back](#)

[Close](#)

[Full Screen / Esc](#)

[Printer-friendly Version](#)

[Interactive Discussion](#)



## Harmonic quiet-day curves as magnetometer baselines

M. van de Kamp

[Title Page](#)

[Abstract](#)

[Introduction](#)

[Conclusions](#)

[References](#)

[Tables](#)

[Figures](#)

[⏪](#)

[⏩](#)

[◀](#)

[▶](#)

[Back](#)

[Close](#)

[Full Screen / Esc](#)

[Printer-friendly Version](#)

[Interactive Discussion](#)



In the context where the effects of the solar disturbances are measured and analysed (e.g. when calculating ionospheric equivalent currents), all magnetic field components due to the inner earth, regular ionospheric variations, and the equipment, should be subtracted from ground-based magnetic field measurements, before further analysis.

In this context, the earth's main magnetic field as well as all the regular variations and system effects in the output data of any magnetometer are here treated together as "baselines", indicating the components to be removed.

(Note however, that the term "baseline" has sometimes also been used in the context of studying  $S_q$  variations, where the term represented the relatively long-term variations. For instance, when Matsushita (1968) referred to the  $S_q$  study by Price and Wilkins (1963), he used the term "base line" for the variations of the midnight field from day to day.)

Although the magnetometer baseline method of this paper is introduced as the basis of calculating ionospheric equivalent currents, this method can also be useful for any other application where either the disturbance magnetic field or the  $S_q$  field is to be analysed.

### 1.4 Baseline removal

A traditional method of removing a baseline from magnetometer data of a particular day, is to look for a magnetically quiet day near the day of interest, and calculate the average value of the magnetic field of this day. This constant value is used as the baseline, and subtracted from the data for the day of interest, leaving only the disturbance field. For instance, Davis and Sugiura (1966) proposed to derive the auroral electrojet index  $AE$  from magnetometer data using this as a baseline method.

Although it has long been known that this way, the  $S_q$  variations are not included in the baseline and will therefore be considered as part of the disturbances, it was considered that these variations are small compared to the disturbance field, and hence the introduced error is relatively small.

## Harmonic quiet-day curves as magnetometer baselines

M. van de Kamp

[Title Page](#)

[Abstract](#)

[Introduction](#)

[Conclusions](#)

[References](#)

[Tables](#)

[Figures](#)

[⏪](#)

[⏩](#)

[◀](#)

[▶](#)

[Back](#)

[Close](#)

[Full Screen / Esc](#)

[Printer-friendly Version](#)

[Interactive Discussion](#)



The magnetically “quiet” days used can be more or less frequent, varying from about one to five quiet days per month. They can be determined in various ways, e.g. based on the variations of the data of each day, or using global magnetic indices as  $Kp$  or  $Dst$ . Also, they can be downloaded directly from a global database ([http://www-app3.gfz-potsdam.de/kp\\_index/definitive.html](http://www-app3.gfz-potsdam.de/kp_index/definitive.html)).

The baseline method using averages of quiet days leads to inaccuracies in the resulting disturbed data in several ways:

1. There may not be any day in the entire month which is completely free from disturbances. In this case, the “quiet” day is not really “quiet” and the data, and even the average value, will still be affected by some disturbance effects.
2. As mentioned above, the diurnal variation of the  $S_q$  field is not included in the baseline and will hence be considered as part of the disturbance field.
3. For two consecutive days, the “nearest” quiet day and therefore the baseline value can be different, and hence the baseline may show a discontinuity at midnight between these two days. If this baseline is subtracted from other data for a period around midnight (e.g. to calculate equivalent ionospheric currents), this may cause an artificial jump in the resulting disturbed data.
4. The magnetometer data generally contain slow variations over the course of several days, months and years, caused by long-term magnetic field variations, but also equipment effects (see Sect. 2.2 for examples of each). As a consequence, the average value of the quiet day may not be representative for that of other days which can be several weeks earlier or later.

In spite of its drawbacks, the abovementioned baseline procedure is still being used in some applications today, mainly because of its simplicity. Alternatively, many studies have also been performed using more elaborate baseline procedures. In particular,  $S_q$  variations (point 2) have been incorporated in baselines by appropriate smoothing of the quiet-day data in one way or the other. Below, a few of the most recent baseline

## Harmonic quiet-day curves as magnetometer baselines

M. van de Kamp

[Title Page](#)

[Abstract](#)

[Introduction](#)

[Conclusions](#)

[References](#)

[Tables](#)

[Figures](#)

[⏪](#)

[⏩](#)

[◀](#)

[▶](#)

[Back](#)

[Close](#)

[Full Screen / Esc](#)

[Printer-friendly Version](#)

[Interactive Discussion](#)



procedures are summarised. It should be emphasised that this is not intended to be a complete review of baseline development, but only to show some examples of the current state of the art.

Janzhura and Troshichev (2008) presented a running automatic method which overcomes some of the problems: point 1 is avoided by looking instead of quiet days, for any quietest bits of data within a 30 day period; point 2 is avoided by only smoothing the quiet daily curve, but retaining the diurnal variations. Point 4 is only reduced, not entirely removed, by averaging all quiet data over the 30-day period.

However, their method retains point 3, and even introduces more discontinuities. Since the smoothed daily baseline is in general at the end of the day not the same as that at the start of the day, a discontinuity becomes more likely to occur at every midnight. This can be seen e.g. from Fig. 5 in the paper by Janzhura and Troshichev (2008) (the values of the curves at the end of the day do not connect to those at the start of the day).

More recently, Stauning (2011) presented another version of the procedure from Janzhura and Troshichev. The main difference with their method is that his method carefully selects data from similar conditions as the day in question, by giving larger weights to quiet data from days close to the day in question, as well as to data from days approximately 27 days (one solar rotation) before and after. This is because he finds the highest correlation coefficients for such displacement periods. This way, his method further reduces point 4 as long as the slow variations are fluctuations over periods of 27 days. In addition, very slow fluctuations are removed separately in his method. However, his method does not take care of unexpected fluctuations, such as instrument drifts over only a few days (see Sect. 2.2). Also, it is not certain whether any midnight discontinuities (due to point 3, or those as introduced by Janzhura and Troshichev) remain.

Gjerloev (2012) described the automatic data preprocessing procedure of the world-wide magnetometer network SuperMAG, which also involves a baseline removal technique. Acknowledging the problems associated with the identification of quiet days, he

## Harmonic quiet-day curves as magnetometer baselines

M. van de Kamp

[Title Page](#)

[Abstract](#)

[Introduction](#)

[Conclusions](#)

[References](#)

[Tables](#)

[Figures](#)

[⏪](#)

[⏩](#)

[◀](#)

[▶](#)

[Back](#)

[Close](#)

[Full Screen / Esc](#)

[Printer-friendly Version](#)

[Interactive Discussion](#)

avoids using these altogether, thus avoiding point 1. Instead, he averages the data from several days around the day of interest (3 days in case of relatively quiet periods; longer in disturbed periods), to obtain a daily trend, and applies appropriate smoothing, avoiding point 2. Point 4 is taken care of by separately determining seasonal variations (referred to as “yearly trend”), although it is not clear how well this works to capture relatively fast and irregular equipment drifts. In addition, also here it is not clear but likely that the midnight discontinuities remain.

In this context it is good to note that all of the above methods were designed to work for rather well-controlled stable instrumentation, in which case point 4 represents only slow and regular variations, which are well taken care of by these methods.

In this paper however, a method is described which overcomes all problems in the list above, including in the case of unstable instrumentation, and in addition is simpler than the other methods described above. The procedure will be described in the next section.

## 2 Procedure

The baseline procedure is performed for each magnetometer station separately. The following sections describe the various steps in this procedure.

### 2.1 Data jumps

Many of the magnetometer time series, especially those from remote unmanned stations, exhibit occasional artificial discontinuities, or “jumps”, in the data. These can vary in size from a few nT to thousands of nT, and can be both positive and negative. The jumps are probably due to adjustments and resetting of the equipment, and happen mostly at midnight, but not only. These jumps, if not taken care of, will affect the results of the data analysis.

## Harmonic quiet-day curves as magnetometer baselines

M. van de Kamp

[Title Page](#)

[Abstract](#)

[Introduction](#)

[Conclusions](#)

[References](#)

[Tables](#)

[Figures](#)

[⏪](#)

[⏩](#)

[◀](#)

[▶](#)

[Back](#)

[Close](#)

[Full Screen / Esc](#)

[Printer-friendly Version](#)

[Interactive Discussion](#)



Small discontinuities in the time series need not be a problem in a statistical analysis of the magnetic field. However, they do become important when dynamics aspects of geomagnetic events are analysed. For example, the results of the time derivative of the magnetic field will be affected by artificial jumps. Viljanen et al. (2001) analysed the time derivative of the horizontal magnetic field vector from the IMAGE network, and found significant correlations between this parameter and geomagnetic activity, on various time scales from hours up to years, as well as a significant directional variability of this parameter, which in turn also depends on location and time. Plausible relations were found with, among other things, ionospheric currents, pulsations, and geomagnetically induced currents. Because of this, it is evidently important to avoid the measured time derivative being contaminated by artificial discontinuities. (For the same reason, the artificial jumps in magnetometer data introduced by the baselines, i.e. problem 3 in Sect. 1.4, should also be avoided.)

Furthermore, the data jumps will also affect the baseline determination described in this paper, which involves, among other things, some curve-fitting and calculation of standard deviations (see later). Because of this, as a first step in the baseline procedure, these jumps need to be removed from the measured data.

The jumps are removed as follows. A software module has been designed which detects and displays suspected discontinuities in the data. The software lets the user examine each discontinuity and decide whether it is artificial, in which case it is listed in a datafile. Based on these data, a jumps-baseline  $B_J(t)$  is generated, separately for the  $x$ - and  $y$ -components of the field, which contains all the jumps found in the data, but is otherwise constant. This jumps-baseline is subtracted from the raw data, before any further processing as described in the following sections.

## 2.2 Long-term baseline

Next, to determine the baseline, first the part is considered which consists of the long-term variations in the magnetic field, i.e. variations over periods longer than 24 h: on the scale of days, months, or years. These variations will be represented in the baseline

by determining from every day of data a single daily “background” value. For this value it might be considered to use the average of the measured data, however, rather than this, the median is considered more stable, being less sensitive to extreme values during moderately disturbed days.

Figure 2 shows this daily median calculated over various periods of data, and demonstrates the long-term variations revealed by it. This graph shows that these variations consist of, among others, the following components:

- *Secular variations*: due to very slow variations in the earth’s internal magnetic field pattern, the  $y$ - and  $z$ - components of the magnetic field at all stations steadily increased, at a rate of slightly over 35 nT per yr, during the period 2001–2010. (The  $x$ -component did not change significantly.) The upper left-hand graph of Fig. 2 demonstrates this for  $B_y$  in Uppsala.
- *Seasonal variations*: the seasonal changes in the ionospheric conductivity and in the ionosphere-thermosphere-magnetosphere interactions result in variations in all magnetic field components with a period length of one year. As an example, the upper right-hand graph of Fig. 2 shows that  $B_x$  in Uppsala oscillated at about 10 nT peak-to-peak within the years of 2008 and 2009.
- *Tidal variations*: variations with periods of about 27 days can be observed, which are the result of interference between  $S_q$  and  $L$  variations. As an example, the lower left-hand graph of Fig. 2 shows that  $B_x$  in Uppsala varied at this frequency at about 15 nT peak-to-peak in October to December 2007. (Note that the raw data, which are also shown (red), include the disturbance field and therefore also show statistical variations due to the period of solar activity changes, which also have a period of 27 days. The median values however should not be much affected by this.)
- *Equipment drift*: some of the magnetometers occasionally exhibit some variations over the course of one or a few days, which do not repeat, and show no correlation

## Harmonic quiet-day curves as magnetometer baselines

M. van de Kamp

[Title Page](#)

[Abstract](#)

[Introduction](#)

[Conclusions](#)

[References](#)

[Tables](#)

[Figures](#)

[⏪](#)

[⏩](#)

[◀](#)

[▶](#)

[Back](#)

[Close](#)

[Full Screen / Esc](#)

[Printer-friendly Version](#)

[Interactive Discussion](#)



## Harmonic quiet-day curves as magnetometer baselines

M. van de Kamp

[Title Page](#)

[Abstract](#)

[Introduction](#)

[Conclusions](#)

[References](#)

[Tables](#)

[Figures](#)

[⏪](#)

[⏩](#)

[◀](#)

[▶](#)

[Back](#)

[Close](#)

[Full Screen / Esc](#)

[Printer-friendly Version](#)

[Interactive Discussion](#)



with space weather parameters or with any of the other magnetometer results. The lower right-hand graph shows an example for Sørøya, where on 23 December 2009, the readings for  $B_x$  decreased by 80 nT over two days, and then gradually recovered, over the course of 18 days.

5 The equipment drifts especially happened at the stations in remote locations, which are not continuously manned and monitored. These drifts should obviously be classified as measurement errors. However, if they can be quantified using the current method, they can be removed along with the above-mentioned long-term variations in the magnetic field, which means that these low-quality data need not be discarded.

10 This is a very useful outcome, since these magnetometer stations in remote places often are some of the most crucial ones. A significant number of them are located in northern Scandinavia and the sea between Norway and Svalbard, which is the area above which the auroral oval or its boundaries are often located, and where therefore much of the magnetic activity occurs. But at the same time, not many magnetometers

15 are present there, due to the difficult accessibility of the area. The resulting relevance of the area is precisely why these particular magnetometers were placed in these locations, despite their inaccessibility. It is therefore very useful if these relatively valuable results, even if not of perfect quality, can still be used in ionospheric analyses.

20 The median is used for the long-term baseline as follows. The median value is calculated for every day of data. The long-term baseline is considered to be equal to the median for 12:00 UT at the respective day. At any other time, the long-term baseline is interpolated between these values. The resulting time-dependent long-term baseline will be referred to in this paper as  $B_T(t)$ . The procedure to determine  $B_T(t)$  is performed separately for each field component (and each different station).

25 Obviously, during magnetically very disturbed periods, the median value calculated over a day may not be representative for the long-term baseline. In these cases, the median of these particular days will not be used, but the long-term baseline will be interpolated between other median values. Further on, it will be shown how the classification of these “usable” median values is performed.

## 2.3 Quiet days

For every separate magnetometer station, a list of the quietest days of each month is generated.

At any magnetometer station, a day is considered “quiet” if the magnetic field variations measured on this day are as much as possible caused by  $S_q$  variations and not by magnetic disturbances driven by solar activity. Hence, a “quiet” day would mainly contain slow variations; its fast variations should be relatively small compared to the slow variations.

Because the fast variations due to disturbances are mostly much larger than the  $S_q$  variations, it seems logical to calculate simply the standard deviation of every day of data, and look for the smallest standard deviations of each month. Indeed this method works reasonably, however there are cases where this method is too coarse, as will become clear in the description below of the method of this paper.

In this paper, the quiet-day selection is performed as follows. Each day of data is partitioned into 24 one-hour sections. In each one-hour section, a straight line is fitted to the data, for the  $x$ - and  $y$ - components of the magnetic field. This straight line is subtracted from the data, and from the remaining data, the hourly standard deviation,  $\sigma_H$ , is calculated. The result of this is  $2 \times 24$  values (2 components and 24 h) of  $\sigma_H$ . Of these 48 values, the daily maximum is calculated, referred to as  $\sigma_{H_{\max}}$ , for each day and each station. These values of  $\sigma_{H_{\max}}$  are the indicators for days with and without disturbances: of each month, the day with the lowest  $\sigma_{H_{\max}}$  is selected as the “quiet day” for that month, at that station.

As an extra requirement, the “quiet day” should contain no data gaps, so only days with 100% data availability for all magnetic components can be potential candidates for any month’s “quiet day”.

Figure 3 demonstrates this procedure, showing  $B_x$  in Oulujärvi on three different days in March 2002. The day shown in the bottom two graphs, 28 March, resulted from this procedure as the quietest day of this month (note that the actual procedure also

## Harmonic quiet-day curves as magnetometer baselines

M. van de Kamp

[Title Page](#)

[Abstract](#)

[Introduction](#)

[Conclusions](#)

[References](#)

[Tables](#)

[Figures](#)

[⏪](#)

[⏩](#)

[◀](#)

[▶](#)

[Back](#)

[Close](#)

[Full Screen / Esc](#)

[Printer-friendly Version](#)

[Interactive Discussion](#)



takes into account the  $y$ -component of the magnetic field, which is not shown in the figure).

Figure 4 demonstrates why this procedure works better than calculating the overall standard deviation of the whole day. On 28 March (the quiet day at the bottom of Fig. 3) the full-day standard deviation of  $B_x$  is 19.9 nT, while on 7 March (Fig. 4), it is smaller: 10.0 nT. However, the latter day contains some small-scale variations, which make it less suitable as a “quiet” day. This property is revealed by the maximum hourly standard deviation  $\sigma_{H_{\max}}$ , which is larger on 7 March: 6.7 nT rather than 1.4 nT.

Of course, even though according to this procedure a “quietest” day of each month can always be found (as long as at least one full day of data is available), it may be that this quietest day still contains too much magnetic disturbance to be used for a quiet day curve. Especially during and around the solar active year of 2003, disturbances can be so frequent, that not necessarily a full day can be found within every month where these disturbances are insignificantly small. In other words: the “quietest” day of the month may not be really “quiet”.

Because of this, an extra criterion is applied: if for any month, the value of  $\sigma_{H_{\max}}$  of the quiet day is above a certain threshold value, then this quiet day is discarded and no quiet day is assigned for this month. Later it will become clear that these cases do not cause a problem in the rest of the procedure. The optimum threshold value of  $\sigma_{H_{\max}}$  to be used for this, depends on the typical level of both slow and fast variations in the magnetic field, and therefore varies from station to station. The values used were optimised empirically; the results are listed for all IMAGE stations in Table 1 (5th column). Using these threshold values, generally no more than three consecutive months without quiet days were encountered for any station in the entire IMAGE database 2001–2010.

## 2.4 Very disturbed days

The information of the hourly standard deviations  $\sigma_H$ , calculated as described in the previous section, will also be used to classify certain days as too disturbed to calculate

## Harmonic quiet-day curves as magnetometer baselines

M. van de Kamp

[Title Page](#)

[Abstract](#)

[Introduction](#)

[Conclusions](#)

[References](#)

[Tables](#)

[Figures](#)

[⏪](#)

[⏩](#)

[◀](#)

[▶](#)

[Back](#)

[Close](#)

[Full Screen / Esc](#)

[Printer-friendly Version](#)

[Interactive Discussion](#)



the median value from, which would be used for determination of the long-term baseline  $B_T(t)$  (see Sect. 2.2).

In the top graph of Fig. 5, three days of  $B_x$ -data from Abisko in November 2001 are shown, along with their daily median values (green stars). On 4 November, conditions are mostly quiet, and the median value is a good representative of the long-term baseline. On 5 November, some disturbances start late in the day, but the median value is not significantly affected by it. However, on 6 November, conditions are disturbed all day, and the median value is dominated by these disturbances, and unsuitable to be used for the long-term baseline.

A rule of thumb can be described as: a median value is relatively insensitive to irregularities in data as long as these irregularities consist of less than half of the data. This can be seen on 5 November in Fig. 5: since the irregularities consist of less than half the day, the median is not significantly affected by them.

Because of this rule, the distribution of hourly standard deviations  $\sigma_H$  can serve as a useful indicator for the stability of the daily median value. If more than half of the day's  $\sigma_H$  values indicate disturbed data during their hours (as in the previous section), it can be assumed that more than half of the data of the day are disturbed, and the daily median value will be unreliable. On the other hand, if more than half of the  $\sigma_H$  values are low, then more than half of the day's data will be quiet, and the median value will be relatively unaffected by any disturbances. These different cases are clearly illustrated in the bottom graph of Fig. 5, where the  $\sigma_H$  values of the data in the upper graph are shown (blue stars).

This criterion is easily represented by the median value of the day's hourly standard deviation, which will be referred to as  $\sigma_{H_{\text{med}}}$ . If  $\sigma_{H_{\text{med}}}$  is above a certain threshold, this means that at least half the  $\sigma_H$  values are above this threshold. This can be seen in the bottom graph of Fig. 5, where  $\sigma_{H_{\text{med}}}$  are the red stars. As a threshold value of  $B_x$  for Abisko, 17 nT was empirically chosen (dashed line in Fig. 5).

The decision whether a median value is used for the long-term baseline  $B_T(t)$  is made separately for  $B_x$  and  $B_y$ . Because typical variations in  $B_y$  are often different from

## Harmonic quiet-day curves as magnetometer baselines

M. van de Kamp

[Title Page](#)

[Abstract](#)

[Introduction](#)

[Conclusions](#)

[References](#)

[Tables](#)

[Figures](#)

[⏪](#)

[⏩](#)

[◀](#)

[▶](#)

[Back](#)

[Close](#)

[Full Screen / Esc](#)

[Printer-friendly Version](#)

[Interactive Discussion](#)





used. These complex values represent the amplitudes and phases of harmonics of frequencies which are all multiples of the inverse of 1 day. The frequencies of the first 7 harmonics are given in Table 2.

The curve, composed of these 7 lowest harmonics of the quiet day, is equivalent to a low-pass filtered version of the quiet-day data. The resulting curve, which will here be called a “template”, will be used as a basis of the baseline construction. The template is described as follows:

$$T(t_d) = \sum_{h=0}^6 |X_h| \cos \left( \frac{2\pi h t_d}{86400} + \arg(X_h) \right) \quad (1)$$

where

$t_d$  = “time of day”; time elapsed since midnight (s)

$h$  = index number of harmonic (0..6)

$X_h$  = (complex) coefficient of harmonic  $h$  (nT).

There will be one set of harmonic coefficients  $X_h$ , and therefore one template  $T(t)$ , defined for each quiet day (and each field component). One example day of data, and the template derived from it, are shown in Fig. 7. Note that, for ease of comparison,  $B_T(t)$  has been subtracted from the data.

It is worth noting that since all the cosine arguments in Eq. (1) cover an exact number of cycles over the length of one day (86 400 s), the template value at midnight at the end of the day, i.e.  $T(86\,400\text{ s})$ , will always be equal to that at midnight at the start,  $T(0\text{ s})$ , thus ensuring continuity at midnight if the template would be used on consecutive days. However, the templates are not used directly as such for the baselines, which will be shown in the next subsection.

## 2.6 Diurnal baseline

As the next step, a curve representing the  $S_q$  variations, i.e. the diurnal variation of the background magnetic field, is derived from the templates, separately for the  $x$ - and

## Harmonic quiet-day curves as magnetometer baselines

M. van de Kamp

[Title Page](#)

[Abstract](#)

[Introduction](#)

[Conclusions](#)

[References](#)

[Tables](#)

[Figures](#)

[⏪](#)

[⏩](#)

[◀](#)

[▶](#)

[Back](#)

[Close](#)

[Full Screen / Esc](#)

[Printer-friendly Version](#)

[Interactive Discussion](#)





days was 66 days of data, over a period of 99 days (Masi station; between 6 February and 17 May 2003).

## 2.7 Full baseline

To obtain the full baseline, the diurnal baseline  $B_S$  is added to the long-term baseline  $B_T$  and the jumps baseline  $B_J$ , separately for the  $x$ - and  $y$ -components:

$$B_B(t) = B_S(t) + B_T(t) + B_J(t) \quad (3)$$

where

$B_B$  = full baseline;

$B_S$  = diurnal baseline, derived from quiet days as described in Sects. 2.3, 2.5 and 2.6;

$B_T$  = long-term baseline, derived from suitable median values as described in Sects. 2.2 and 2.4;

$B_J$  = jumps-baseline, containing only the data jumps as described in Sect. 2.1.

Figure 9 presents an example of the result of the procedure described in this section. It shows the  $B_x$ -field in Uppsala from 22 March to 10 April in 2005 (two quiet days), and the corresponding baseline. In this example, the diurnal variation of the baseline follows that of the data not only on the assigned quiet days, but also on relatively quiet intervals in the middle of this period (e.g. 1 April). Furthermore, the long-term (mostly tidal) variation of the data is well followed by the baseline.

Figure 10 shows an example for the  $B_x$ -field in December 2009 in Sørøya, which experienced some significant equipment drift in this period (also shown in Fig. 3). The figure shows that the baseline derived for this period follows the equipment drift well, making this data reasonably usable for equivalent current calculations.

## Harmonic quiet-day curves as magnetometer baselines

M. van de Kamp

[Title Page](#)

[Abstract](#)

[Introduction](#)

[Conclusions](#)

[References](#)

[Tables](#)

[Figures](#)

[⏪](#)

[⏩](#)

[◀](#)

[▶](#)

[Back](#)

[Close](#)

[Full Screen / Esc](#)

[Printer-friendly Version](#)

[Interactive Discussion](#)





## Harmonic quiet-day curves as magnetometer baselines

M. van de Kamp

[Title Page](#)

[Abstract](#)

[Introduction](#)

[Conclusions](#)

[References](#)

[Tables](#)

[Figures](#)

[⏪](#)

[⏩](#)

[◀](#)

[▶](#)

[Back](#)

[Close](#)

[Full Screen / Esc](#)

[Printer-friendly Version](#)

[Interactive Discussion](#)



The distribution using the smoothed curves of the quiet days is also more spread for small values than the one using the harmonic baseline, but not quite as much as the one using the quiet-day averages. This must be due to variations in the  $S_q$  field from day to day (such as the tidal variations described in Sect. 7). These variations are excluded from the baseline if the same daily curve is used for the entire month, and are therefore included in the disturbance field, which again causes the pdf to spread small values over a larger range.

Apart from that, some other features are seen in the graph, which are most pronounced in those stations which are relatively little monitored. In particular, the pdf of the  $B_x$ -field in Nordkapp shows some unrealistic peaks at  $B_x = -55, 90$  and  $200$  nT, both when the quiet-day averages are used as baseline and when the LPF-filtered quiet-day curves are used. Apparently, some extended periods exist in the database where the disturbance field varies unrealistically around a nonzero value, obviously due to the fact the the quiet day is not realistic as a baseline, either averaged or smoothed. The pdf of the disturbance field using the harmonic baseline as described in this paper does not show these artifacts, and presents a realistic function all the way.

As another example, the pdf of the  $B_x$ -field in Karmøy is shown in Fig. 12 using the same three methods. This figure shows an even stronger peak around  $-130$  nT when the quiet day averages or the smoothed quiet-day curves are used as baselines, due to the same cause as above.

It should be emphasised here, that the baseline methods by Janzhura and Troshichev (2008), Stauning (2011), and Gjerloev (2011) are all better than the two methods used here for comparison. They would likely include all diurnal  $S_q$  and longer-term variations in the baseline, resulting in an equally sharp peak around zero for the pdf of the disturbed field as the blue line in Figs. 11 and 12. However, these methods are not likely to deal with equipment effects efficiently, which makes it likely that the resulting pdf of the disturbance field would show similar unrealistic peaks as the red and green curves in the graphs of this section. (In addition, these methods would leave

discontinuities in the disturbance field, as explained in Sect. 1.4; this is a feature which does not show up in the pdf curve.)

## 4 Other applications

Now that the harmonic coefficients  $X_h$  (in e.g. Eq. 1) and  $Y_h$  of the magnetometer baselines have been derived over 10 yr and for 32 magnetometer stations, these can be used to examine their long-term behaviour, which represent the Solar quiet-time ( $S_q$ ) diurnal variation of the magnetic field  $B_x$  and  $B_y$ . Like the disturbance field, also this field is mainly caused by currents in the ionosphere. However, unlike the disturbance field, this field varies with diurnal variations of electron density in the ionosphere, which in turn depends on solar radiation.

Several statistical studies of the harmonic coefficients of  $S_q$  diurnal variations, dependent on season, year, location and solar activity, have already been made throughout the 20th century, revealing information about the long-term dependencies of the geomagnetic field, see e.g. the overviews by Matsushita (1968) and Campbell (1989). The results obtained in the study of the current paper can help to verify those studies, and help to improve prediction models of the  $S_q$  magnetic field. This will be the subject of a later paper.

## 5 Conclusions

A novel method of determining the baselines of magnetometer data has been presented. The full baseline is composed of three components:

- A jump baseline, which contains only the artificial jumps in the data and is otherwise constant.
- A long-term baseline, interpolated between daily median values of the raw data of most days. The daily median values are calculated for all days except the most

## Harmonic quiet-day curves as magnetometer baselines

M. van de Kamp

[Title Page](#)

[Abstract](#)

[Introduction](#)

[Conclusions](#)

[References](#)

[Tables](#)

[Figures](#)



[Back](#)

[Close](#)

[Full Screen / Esc](#)

[Printer-friendly Version](#)

[Interactive Discussion](#)



**Harmonic quiet-day curves as magnetometer baselines**

M. van de Kamp

<a href="#">Title Page</a>	
<a href="#">Abstract</a>	<a href="#">Introduction</a>
<a href="#">Conclusions</a>	<a href="#">References</a>
<a href="#">Tables</a>	<a href="#">Figures</a>
<a href="#">⏪</a>	<a href="#">⏩</a>
<a href="#">◀</a>	<a href="#">▶</a>
<a href="#">Back</a>	<a href="#">Close</a>
<a href="#">Full Screen / Esc</a>	
<a href="#">Printer-friendly Version</a>	
<a href="#">Interactive Discussion</a>	

disturbed ones; a procedure is included to ensure that these median values are unaffected by disturbances.

- A diurnal baseline, interpolated between “templates”, i.e. diurnal baselines of the nearest two quiet days. These templates consist of the first seven harmonics of the diurnal variation of the magnetic field of the quiet days. This method ensures a smooth baseline at all times, avoiding any discontinuities at transitions between days or months.

More than the traditional method of using the average of the nearest quiet day as a baseline, the baseline derived according to this method is able to follow medium-to-long-term variations in the measured magnetic field, such as tidal and secular variations, as well as equipment drifts of individual instruments. The procedure avoids many problems associated with other existing baseline procedures, and makes magnetometer data suitable for the calculation of ionospheric equivalent currents. Even data from remote unmanned magnetometers, which exhibit significant equipment effects, can be made suitable with this method, which can give valuable contributions to the equivalent current database.

*Acknowledgements.* The research leading to these results has received funding from the European Community’s Seventh Framework Programme (FP7/2007-2013) within the call for “Exploitation of Space Science and Exploration Data”, under grant agreement no. 263325 (ECLAT project).

The author would like to thank the institutes who maintain the IMAGE Magnetometer network.

**References**

Amm, O. and Viljanen, A.: Ionospheric disturbance magnetic field continuation from the ground to the ionosphere using spherical elementary current systems, *Earth Planet. Space*, 51, 431–440, 1999.

Boteler, D. H., Pirjola, R. J., and Nevanlinna, H.: The effects of geomagnetic disturbances on electrical systems at the earth’s surface, *Adv. Space Res.*, 22, 17–27, 1998.



Discussion Paper | Discussion Paper | Discussion Paper | Discussion Paper | Discussion Paper

## Harmonic quiet-day curves as magnetometer baselines

M. van de Kamp

[Title Page](#)

[Abstract](#)

[Introduction](#)

[Conclusions](#)

[References](#)

[Tables](#)

[Figures](#)

[⏪](#)

[⏩](#)

[◀](#)

[▶](#)

[Back](#)

[Close](#)

[Full Screen / Esc](#)

[Printer-friendly Version](#)

[Interactive Discussion](#)



- Campbell, W. H.: An Introduction to Quiet Daily Geomagnetic Fields, *Pure Appl. Geophys.*, 131, 315–331, 1989.
- Chapman, S. and Bartels, J.: *Geomagnetism*, Clarendon Press, Oxford, UK, 1940.
- Davis, T. N. and Sugiura, M.: Auroral electrojet activity index AE and its universal time variations, *J. Geophys. Res.*, 71, 785–801, 1966.
- Gjerloev, J. W.: The SuperMAG data processing technique, *J. Geophys. Res.*, 117, A09213, doi:10.1029/2012JA017683, 2012.
- Janzhura, A. S. and Troshichev, O. A.: Determination of the running quiet daily geomagnetic variation, *J. Atmos. Sol.-Terr. Phys.*, 70, 962–972, doi:10.1016/j.jastp.2007.11.004, 2008.
- Kamide, Y. and Baumjohann, W.: *Magnetosphere–Ionosphere Coupling, Physics and chemistry in space planetology*, vol. 23, Springer-Verlag, New York, 178 pp., 1993.
- Laakso, H., Perry, C., McCaffrey, S., Herment, D., Allen, A. J., Harvey, C. C., Escoubet, C. P., Gruenberger, C., Taylor, M. G. G. T., and Turner, R.: Cluster Active Archive: Overview, in: *The Cluster Active Archive*, edited by: Laakso, H., Taylor, M. G. T. T., and Escoubet, C. P., *Astrophysics and Space Science Proceedings*, Springer, doi:10.1007/978-90-481-3499-1\_1, 2009.
- Matsushita, S.: *Sq and L Current Systems in the Ionosphere*, *Geophys. J. Astr. Soc.*, 15, 109–125, 1968.
- Pedatella, N. M., Forbes, J. M., and Richmond, A. D.: Seasonal and longitudinal variations of the solar quiet (*Sq*) current system during solar minimum determined by CHAMP satellite magnetic field observations, *J. Geophys. Res.*, 116, A04317, doi:10.1029/2010JA016289, 2011.
- Price, A. T. and Wilkins, G. A.: New methods for the analysis of geomagnetic fields and their application to the *Sq* field of 1932–33, *Philos. T. Roy. Soc. A*, 156, 31–98, 1963.
- Pulkkinen, A., Amm, O., Viljanen, A., and BEAR Working Group: Ionospheric equivalent current distributions determined with the method of spherical elementary current systems, *J. Geophys. Res.*, 108, 1053, doi:10.1029/2001JA005085, 2003.
- Stauning, P.: Determination of the quiet daily geomagnetic variations for polar regions, *J. Atmos. Sol.-Terr. Phys.*, 73, 2314–2330, doi:10.1016/j.jastp.2011.07.004, 2011.
- Sugiura, M.: Hourly values of equatorial Dst for the IGY, *Annals of the International Geophysical Year*, Vol. XXXV, Part I, International Council of Scientific Unions, Pergamon Press, 9–45, 1964.

Untiedt, J. and Baumjohann, W.: Studies of polar current systems using the IMS Scandinavian magnetometer array, Space Sci. Rev., 63, 245–390, 1993.

Viljanen, A. and Häkkinen, L.: IMAGE magnetometer network, in: Satellite-Ground Based Co-ordination Sourcebook, edited by: Lockwood, M., Wild, M. N., and Opgenoorth, H. J., ESA publications SP-1198, ESTEC, Noordwijk, the Netherlands, 111–117, 1997.

5 Viljanen, A., Nevanlinna, H., Pajunpää, K., and Pulkkinen, A.: Time derivative of the horizontal geomagnetic field as an activity indicator, Ann. Geophys., 19, 1107–1118, doi:10.5194/angeo-19-1107-2001, 2001.

## GID

3, 87–125, 2013

### Harmonic quiet-day curves as magnetometer baselines

M. van de Kamp

Title Page

Abstract

Introduction

Conclusions

References

Tables

Figures

⏪

⏩

◀

▶

Back

Close

Full Screen / Esc

Printer-friendly Version

Interactive Discussion



**Table 1.** Threshold values of  $\sigma_{H_{\max}}$  and  $\sigma_{H_{\text{med}}}$  for each IMAGE station.

Station	Name	latitude (°)	longitude (°)	Threshold $\sigma_{H_{\max}}$ (nT)	Threshold $\sigma_{H_{\text{med}}}, B_x$ (nT)	Threshold $\sigma_{H_{\text{med}}}, B_y$ (nT)
NAL	Ny Ålesund	78.92	11.95	18	14	13
LYR	Longyearbyen	78.20	15.82	21	16	15
HOR	Hornsund	77.00	15.60	25	20	17
HOP	Hopen Island	76.51	25.01	29	22	14
BJN	Bjørnøya	74.50	19.20	28	21	15
NOR	Nordkapp	71.09	25.79	19	25	12
SOR	Sørøya	70.54	22.22	20	20	12
KEV	Kevo	69.76	27.01	14	18	9
TRO	Tromsø	69.66	18.94	17	20	11
MAS	Masi	69.46	23.70	13	18	11
AND	Andenes	69.30	16.03	17	20	11
KIL	Kilpisjärvi	69.06	20.77	13	18	10
IVA	Ivalo	68.56	27.29	10	16	8
ABK	Abisko	68.35	18.82	11	17	10
LEK	Leknes	68.13	13.54	10	15	9
MUO	Muonio	68.02	23.53	9	15	8
LOZ	Lovozero	67.97	35.08	8	12	6
KIR	Kiruna	67.84	20.42	9	14	8
SOD	Sodankylä	67.37	26.63	8	13	7
PEL	Pello	66.90	24.08	7	12	7
DON	Dønna	66.11	12.50	7	11	6
RVK	Rørvik	64.94	10.98	6	9	5
LYC	Lycksele	64.61	18.75	8	19	7
OUJ	Oulujärvi	64.52	27.23	6	7	5
MEK	Mekrijärvi	62.77	30.97	5	4	4
HAN	Hankasalmi	62.25	26.60	5	4	4
DOB	Dombås	62.07	9.11	4	5	4
SOL	Solund	61.08	4.84	4	4	4
NUR	Nurmijärvi	60.50	24.65	4	5	3
UPS	Uppsala	59.90	17.35	4	4	3
KAR	Karmøy	59.21	5.24	4	3	3
TAR	Tartu	58.26	26.46	4	3	3

**Harmonic quiet-day  
curves as  
magnetometer  
baselines**

M. van de Kamp

[Title Page](#)

[Abstract](#)

[Introduction](#)

[Conclusions](#)

[References](#)

[Tables](#)

[Figures](#)

[⏪](#)

[⏩](#)

[◀](#)

[▶](#)

[Back](#)

[Close](#)

[Full Screen / Esc](#)

[Printer-friendly Version](#)

[Interactive Discussion](#)



## GID

3, 87–125, 2013

## Harmonic quiet-day curves as magnetometer baselines

M. van de Kamp

**Table 2.** Frequencies of the 7 lowest harmonics of data of 1 day.

harmonic nr.	$f$ (Hz)	period
0	0	inf
1	$1.1574 \times 10^{-5}$	1 day
2	$2.3148 \times 10^{-5}$	12 h
3	$3.4722 \times 10^{-5}$	8 h
4	$4.6296 \times 10^{-5}$	6 h
5	$5.7870 \times 10^{-5}$	4 h, 48 min
6	$6.9444 \times 10^{-5}$	4 h

[Title Page](#)
[Abstract](#)
[Introduction](#)
[Conclusions](#)
[References](#)
[Tables](#)
[Figures](#)
[⏪](#)
[⏩](#)
[◀](#)
[▶](#)
[Back](#)
[Close](#)
[Full Screen / Esc](#)
[Printer-friendly Version](#)
[Interactive Discussion](#)


## Harmonic quiet-day curves as magnetometer baselines

M. van de Kamp

[Title Page](#)

[Abstract](#)

[Introduction](#)

[Conclusions](#)

[References](#)

[Tables](#)

[Figures](#)

⏪

⏩

◀

▶

[Back](#)

[Close](#)

[Full Screen / Esc](#)

[Printer-friendly Version](#)

[Interactive Discussion](#)

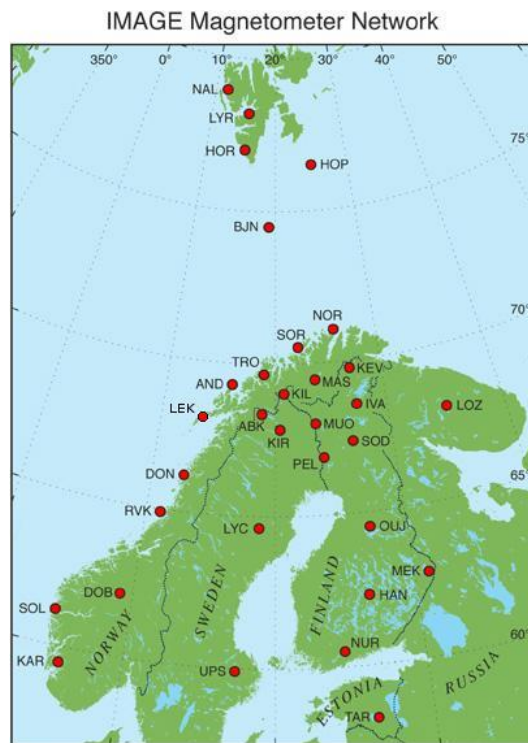


**Fig. 1.** Map of the IMAGE magnetometer stations.

## Harmonic quiet-day curves as magnetometer baselines

M. van de Kamp

[Title Page](#)

[Abstract](#)

[Introduction](#)

[Conclusions](#)

[References](#)

[Tables](#)

[Figures](#)

[⏪](#)

[⏩](#)

[◀](#)

[▶](#)

[Back](#)

[Close](#)

[Full Screen / Esc](#)

[Printer-friendly Version](#)

[Interactive Discussion](#)

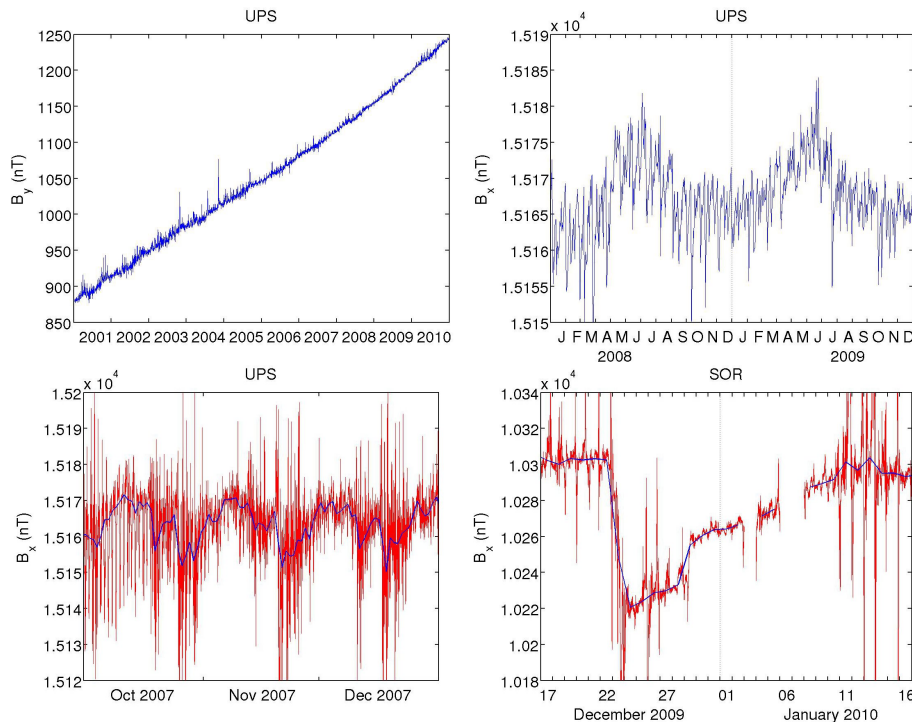


**Fig. 2.** Daily median values of magnetometer data (blue), demonstrating the long-term variations. Top left panel: secular variation in  $B_y$  in Uppsala over the full 10-yr period; top right panel: seasonal variations in  $B_x$  in Uppsala over 2008–2009; bottom left panel: tidal effects in  $B_x$  in Uppsala in autumn 2007 (raw data included in red); bottom right panel: equipment drift in  $B_x$  in Sørøya in December 2009 (raw data in red).

## Harmonic quiet-day curves as magnetometer baselines

M. van de Kamp

[Title Page](#)

[Abstract](#)

[Introduction](#)

[Conclusions](#)

[References](#)

[Tables](#)

[Figures](#)

[⏪](#)

[⏩](#)

[◀](#)

[▶](#)

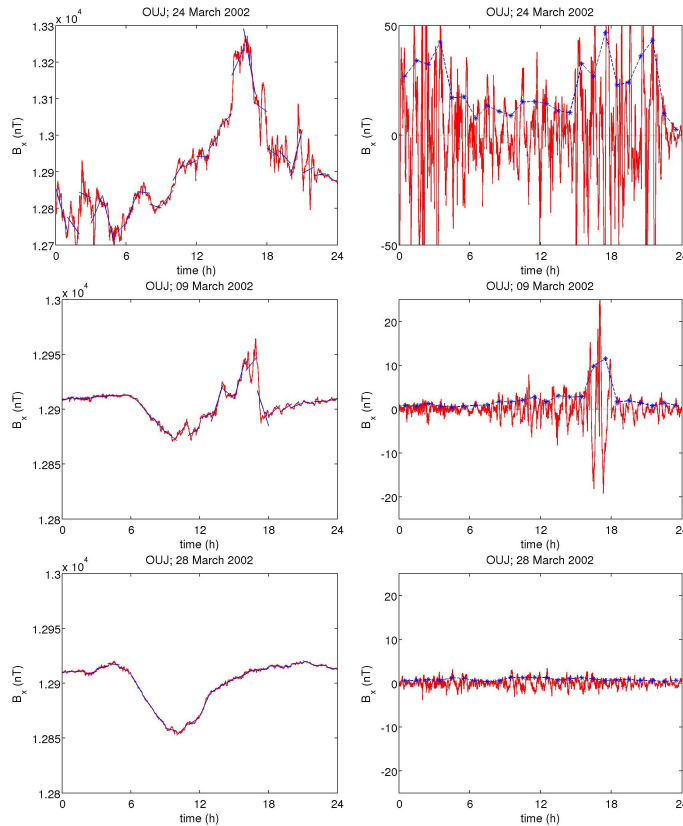
[Back](#)

[Close](#)

[Full Screen / Esc](#)

[Printer-friendly Version](#)

[Interactive Discussion](#)

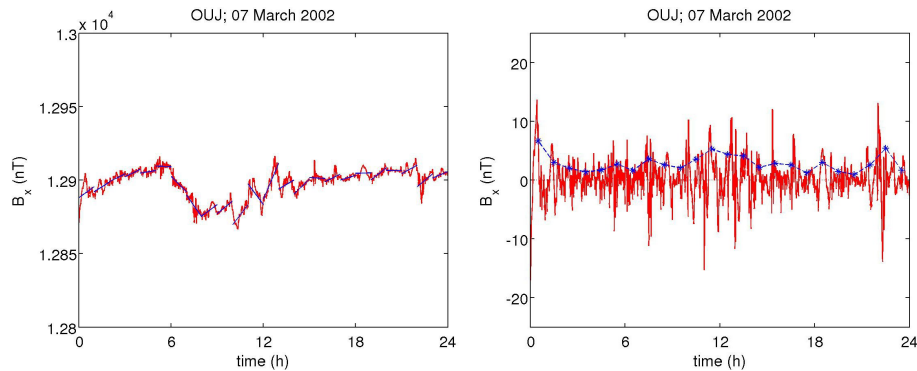


**Fig. 3.** The quiet day selection procedure, demonstrated by the  $B_x$ -field in Oulujärvi in March 2002. Left-hand panels: raw data and the hourly fitted lines fitted to it. Right-hand panels: the data after subtraction of the fitted lines, and the calculated hourly standard deviations. Top panels: on a disturbed day; center: on a mostly quiet day with some disturbance; bottom panels: on a quiet day. The maximum  $\sigma_H$  values (from  $B_x$  alone) are: 46.7, 11.5 and 1.4 nT, respectively.

---

**Harmonic quiet-day curves as magnetometer baselines**M. van de Kamp

---

[Title Page](#)[Abstract](#)[Introduction](#)[Conclusions](#)[References](#)[Tables](#)[Figures](#)[⏪](#)[⏩](#)[◀](#)[▶](#)[Back](#)[Close](#)[Full Screen / Esc](#)[Printer-friendly Version](#)[Interactive Discussion](#)

**Fig. 4.** Similar panels as in Fig. 3, for 7 March 2002, which, although the overall variations are quite small, contains some disturbances. The maximum value of  $\sigma_H$  (from  $B_x$ ) is 6.7 nT.

## Harmonic quiet-day curves as magnetometer baselines

M. van de Kamp

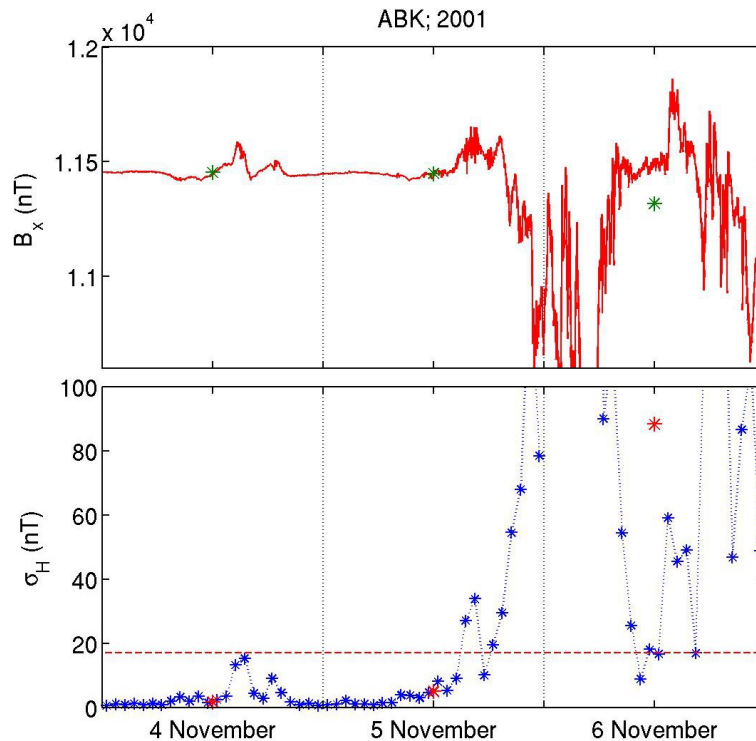


**Fig. 5.** Top panels:  $B_x$  in Abisko on 4–6 November 2001, and the daily median values calculated from it (green stars). Bottom graph: hourly standard deviations  $\sigma_H$  of these data (blue stars), daily medians  $\sigma_{H_{med}}$  of these (red stars), and suggested threshold value for  $\sigma_{H_{med}}$  of  $B_x$  in Abisko (red dashed line).

## Harmonic quiet-day curves as magnetometer baselines

M. van de Kamp

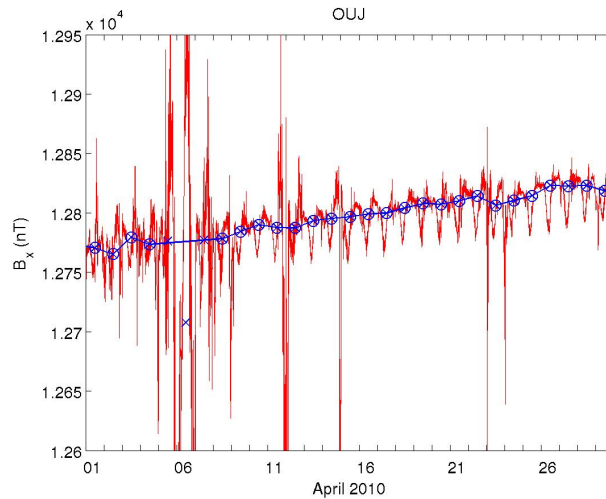


**Fig. 6.**  $B_x$ -field in Oulujärvi in April 2010 (red), the daily median values (blue x), the ones of these that are qualified to be used for the long-term baseline (circles), and this baseline  $B_T(t)$  (blue solid line).

[Title Page](#)[Abstract](#)[Introduction](#)[Conclusions](#)[References](#)[Tables](#)[Figures](#)[⏪](#)[⏩](#)[◀](#)[▶](#)[Back](#)[Close](#)[Full Screen / Esc](#)[Printer-friendly Version](#)[Interactive Discussion](#)

---

## Harmonic quiet-day curves as magnetometer baselines

M. van de Kamp

---

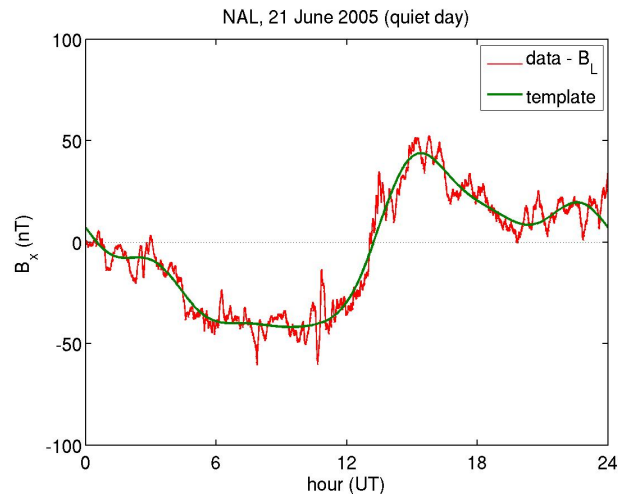


**Fig. 7.** Red:  $B_x$ -field measured by the magnetometer in Ny-Ålesund (NAL) on 21 June 2005, one of the assigned quiet days, with the long-term baseline subtracted, leaving only the diurnal variation. Green: the template derived from this quiet day.

[Title Page](#)[Abstract](#)[Introduction](#)[Conclusions](#)[References](#)[Tables](#)[Figures](#)[⏪](#)[⏩](#)[◀](#)[▶](#)[Back](#)[Close](#)[Full Screen / Esc](#)[Printer-friendly Version](#)[Interactive Discussion](#)

## Harmonic quiet-day curves as magnetometer baselines

M. van de Kamp

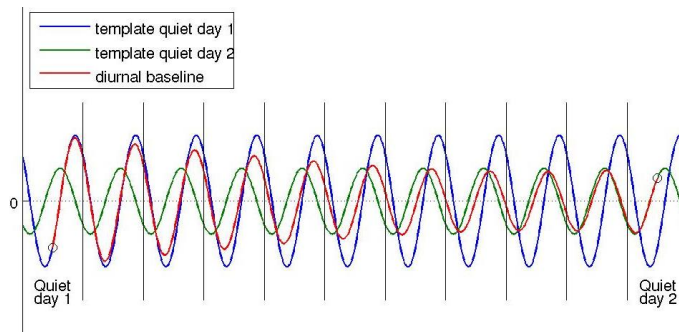


**Fig. 8.** The principle of interpolation between templates. Templates derived from two consecutive quiet days, and the diurnal baseline, interpolated between them. The vertical lines mark midnights (separation between days).

[Title Page](#)[Abstract](#)[Introduction](#)[Conclusions](#)[References](#)[Tables](#)[Figures](#)[⏪](#)[⏩](#)[◀](#)[▶](#)[Back](#)[Close](#)[Full Screen / Esc](#)[Printer-friendly Version](#)[Interactive Discussion](#)

---

## Harmonic quiet-day curves as magnetometer baselines

M. van de Kamp

---

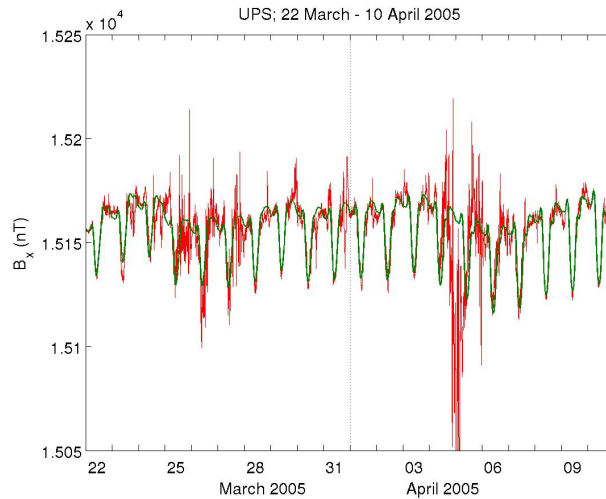


**Fig. 9.**  $B_x$ -field at Uppsala from 22 March to 10 April 2005 (red), and the corresponding baseline derived as described in this paper (green).

[Title Page](#)[Abstract](#)[Introduction](#)[Conclusions](#)[References](#)[Tables](#)[Figures](#)[⏪](#)[⏩](#)[◀](#)[▶](#)[Back](#)[Close](#)[Full Screen / Esc](#)[Printer-friendly Version](#)[Interactive Discussion](#)

---

## Harmonic quiet-day curves as magnetometer baselines

M. van de Kamp

---

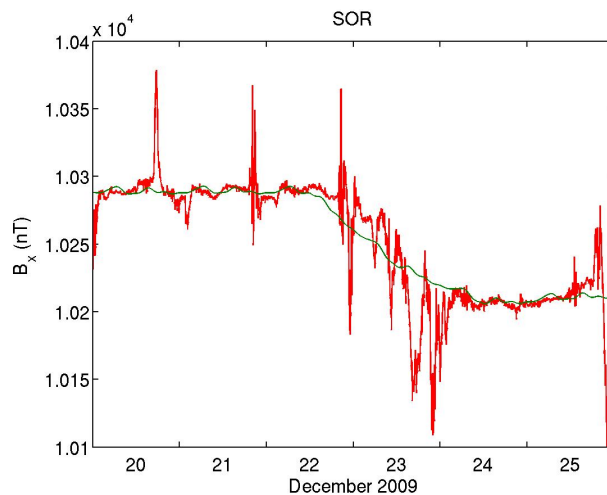


**Fig. 10.**  $B_x$ -field at Sørøya from 20 to 25 December 2009, and the corresponding baseline derived as described in this paper.

[Title Page](#)[Abstract](#)[Introduction](#)[Conclusions](#)[References](#)[Tables](#)[Figures](#)[⏪](#)[⏩](#)[◀](#)[▶](#)[Back](#)[Close](#)[Full Screen / Esc](#)[Printer-friendly Version](#)[Interactive Discussion](#)

## Harmonic quiet-day curves as magnetometer baselines

M. van de Kamp

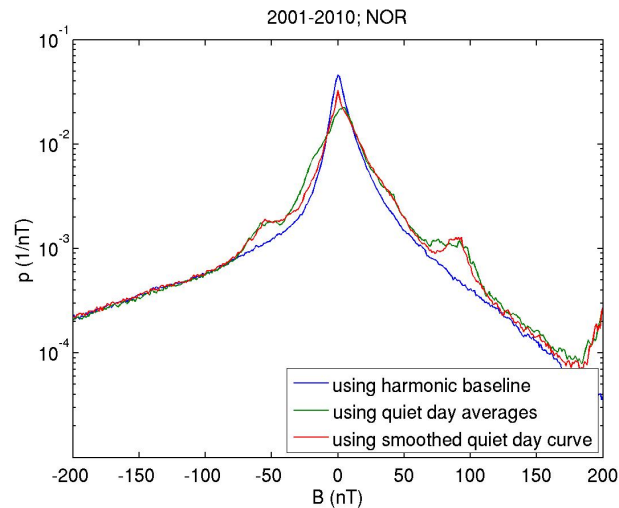


**Fig. 11.** Probability density function of disturbance  $B_x$ -field at Nordkapp over the entire period of 2001–2010, using the harmonic baseline as described in this paper (blue), with the monthly quiet day averages as baseline (green) and with moving-average filtered quiet-day curves as baseline (red).

[Title Page](#)[Abstract](#)[Introduction](#)[Conclusions](#)[References](#)[Tables](#)[Figures](#)[⏪](#)[⏩](#)[◀](#)[▶](#)[Back](#)[Close](#)[Full Screen / Esc](#)[Printer-friendly Version](#)[Interactive Discussion](#)

## Harmonic quiet-day curves as magnetometer baselines

M. van de Kamp

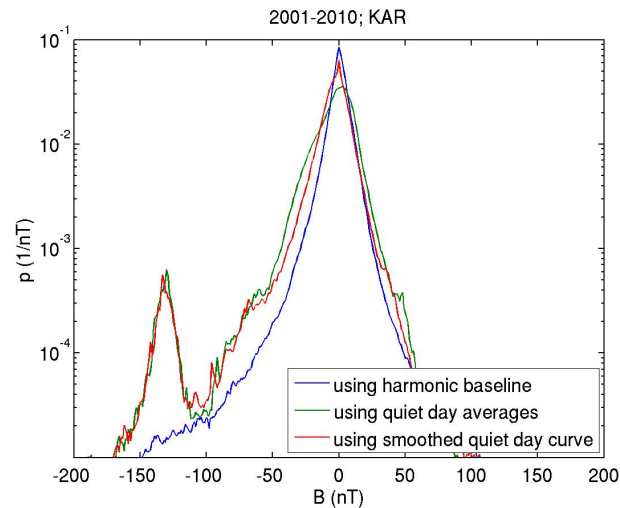


**Fig. 12.** Probability density function of disturbance  $B_x$ -field at Karmøy over the entire period of 2001–2010, using the harmonic baseline as described in this paper (blue), with the monthly quiet day averages as baseline (green) and with moving-average filtered quiet-day curves as baseline (red).

[Title Page](#)[Abstract](#)[Introduction](#)[Conclusions](#)[References](#)[Tables](#)[Figures](#)[⏪](#)[⏩](#)[◀](#)[▶](#)[Back](#)[Close](#)[Full Screen / Esc](#)[Printer-friendly Version](#)[Interactive Discussion](#)